Proceedings of the
International Conference on Mechanical Engineering 2007
(ICME2007) 29- 31 December 2007, Dhaka, Bangladesh

ICME07-FL-05

LIFT ANALYSIS OF AN AIRCRAFT MODEL WITH AND WITHOUT WINGLET

A. Hossain[1], P.R. Arora[2], A.A. Jaafar[2], A.K.M.P. Iqbal[1], M. Arifin[1]

[1]Department of Mechanical Engineering, Faculty of Engineering,
University Industri Selangor, Bestrai Jaya Campus, 45600, Selangor, Malaysia,
[2]Department of Aerospace Engineering, University Putra Malaysia, Malaysia.

ABSTRACT

In order to improve the aerodynamic performance of an aircraft as well as reduction of the required fuel consumption of the commercial aircraft, wingtip device must be properly designed to diffuse the strong vortices produced at the tip and thereby optimise the span wise lift distribution. Based on the previous researches and developments of wing tip devices for the aircraft, winglets have been developed. This paper describes the influences of two pair of elliptical and circular shaped winglets with the wing of the aircraft model for the reduction of induced drag without increasing the span of the aircraft. Aerodynamic characteristics for the aircraft model with and without winglet having wing with NACA section No. 65-3-218 has been studied using a subsonic wind tunnel of 1m × 1m rectangular test section. Lift measurement has been carried out using a six component external balance. Experiments have been carried out on the aircraft model with and without winglet at the Reynolds numbers 0.17×10^6, 0.21×10^6 and 0.25×10^6. The experimental results show that lift curve slope increases by 1-6% with the addition of certain winglet configurations as compared to the aircraft model with and without winglet for the maximum Reynolds number considered in the present study.

Keywords: Winglet, External balance, Lift curve slope.

1. INTRODUCTION

For a number of years many investigations have been carried out to prove the possible benefits of modifying wing tip flow. The aerodynamic performance of an aircraft can be improved by a wingtip device which diffuses the strong vortices produced at the tip and thereby optimize the span wise lift distribution, while maintaining the additional moments on the wing within certain limits. For this purpose the researchers have been doing experiments to produce favorable effects of the flow field using wing tip and reducing the strength of the trailing vortex with the aid of wingtip devices, e.g., winglets, wing tips of complex plan-form, sails, and various modifications of the wingtip side edge. The winglet is cambered and twisted so that the rotating vortex flow at the wing tip creates a lift force on the winglet.

From the beginning of aviation era, designers were searching for methods and technologies for reducing the required fuel consumption of the commercial aircraft. Wingtip devices aimed at the reduction of induced drag, which was responsible for 30-40% of the total drag of a transport-aircraft at long-range cruise condition and for considerably downgrading the climb performance of an aircraft [1]. Winglet alongside with tip tanks, raked wingtips, and aligned fans are belonged to this class of devices.

Modern interest in winglets spans the last 25 years. In July 1976, Richard Whitcomb of NASA Langely Research Centre published a general design approach that summarized the aerodynamic technology involved in winglet design. Small and nearly vertical fins were installed on a KC-135A and flights were tested in 1979 and 1980 [2-3]. Whitcomb showed that winglets could increase an aircraft's range by as much as 7% at cruise speeds. A NASA contract [4] in the 1980s assessed winglets and other drag reduction devices, and are designed as an integral part of the wing.

The "spiroid" wingtip [5] produces a reduction in induced drag at the same time blended winglet [6] reduces drag by eliminating the discontinuity between the wing tip and the winglet. A smoothed version is used on the gently upswept winglet of the Boeing 737-400. Boeing Business Jets and Aviation Partners, Inc. have embarked upon a cooperative program to market conventional winglets for retrofit to the Boeing 7xx series of jetliners. Flight tests on the Boeing Business Jet 737-400 resulted in a 7% drag reduction. Theoretical predictions had indicated that the configuration would have only a 1-2% improvement of drag reduction, and wind tunnel tests had shown only 2% drag reduction [7]. This indicates that wind tunnel test results of winglet configurations should be reviewed with some caution.

The advantages of single winglets for small transport aircraft were investigated by Jones [8], on which they can provide 10% reduction in induced drag compared with

elliptical wings. Winglets are being incorporated into most new transport aircraft, including the Gulfstream III and IV business jets [9], the Boeing 747-400 and McDonnell Douglas MD-11 airliners, and the McDonnell Douglas C-17 military transport. The first industry application of the winglet concept was in wingtip sail. The Pennsylvania State University (PSU) 94-097 airfoil has been designed for use on winglets of high-performance sailplanes [10]. To validate the design codes, as well as the design itself, the airfoil was tested in the Penn State Low-Speed, Low-Turbulence Wind Tunnel from Reynolds numbers of 0.24×10^6 to 1.0×10^6. Performance predictions from two well-known computer codes are compared to the data obtained experimentally, and both are found to generate results that are in good agreement with the wind tunnel measurements.

Another investigation was carried out on wing tip airfoils by J. J. Spillman at the Cranfield Institute of Technology in England [11]. He investigated the use of one to four sails on the wingtip fuel tank of a Paris MS 760 Trainer Aircraft. The flight test results confirmed the wind tunnel test results and demonstrated shorter takeoff rolls and reduced fuel consumption [12]. Spillman later investigated wingtip vortex reduction due to wing tip sails, and found lower vortex energy 400-700 m behind the aircraft, although the rate of decay beyond that was somewhat lower [13].

There has been limited investigation of multiple winglets for aircraft. The split-tip design [14] by Heinz Klug for an aircraft wing is considered a primitive multiple winglets which was created to exploit the non-planar wake geometry by reducing induced drag and wing stress. A biologist with an aerodynamic background has done extensive investigation of the split wingtips of soaring birds and he demonstrated that the tip slots of soaring birds reduce induced drag and increase the span factor of the wings [15]. He found remarkable improvements of slotted wingtips compared with conventional wing with a Clark Y airfoil and he investigated that with the same increase in angle of attack, the Clark Y airfoil tip increased the base wing drag by 25%, while the feathered tip actually reduced the drag by 6%.

To improve the performance of a wing, the multi-winglet [16] design was evaluated to demonstrate its advanced performance potential over the baseline wing and an equivalent single winglet. The results show that certain multi-winglet configurations reduced the wing induced drag and improved L/D by 15-30% compared with the NACA 0012 wing section. In Europe, an extension to the wing tip airfoils has been developed called Wing-Grid [17]. Wing-Grid is a set of multiple wing extensions added to the wing. These small wings are added at various angles so that their tip vortices do not interact to form a strong vortex. These smaller vortices dissipate the vortex energy so that the lift distribution is modified and the induced drag of the wing is reduced. But this concept is limited, since it is not able to change configuration in flight to optimize drag reduction.

Aerodynamic characteristics for the aircraft model with and without winglet having wing with NACA section No. 65-3-218 has been presented in this paper. The study on the enhanced performance of the aircraft models is also given by incorporating elliptical and circular winglets. An interaction matrix method has also been presented to revalidate the calibration matrix data provided by the manufacturer of the six-component external balance. The calibration of free stream velocity and flow quality in the test section has been established and documented.

2. METHODOLOGY

2.1 Speed calibration

Subsonic wind tunnel of 2.5m length, 1m width and 1m height rectangular test section at the Aerodynamics Laboratory of the Aerospace Engineering Department, University Putra Malaysia is used for carrying out the experiments. The ambient pressure, temperature and humidity are recorded using barometer, thermometer, and hygrometer respectively for the evaluation of air density in the laboratory environment.

The airflow velocity is controlled by the RPM controller of the wind tunnel. For the different Hz settings at the RPM controller the flow velocities in wind tunnel test section are recorded using six-component external balance software. In addition to this dynamic pressure at the pitot tube is recorded with digital manometer and corresponding velocities are calculated [18] (Table 1). The validity of the digital manometer was confirmed by comparing the dynamic pressure measured through the digital manometer and through the tube manometer used along with the pitot tube mounted in the test section. The flow velocity versus RPM controller speed curves is plotted for the data obtained through six components external balance software, digital manometer and tube manometer and are given in figure-1. Least square fit lines are drawn through the data and the corresponding lines are given in figure-1.

Table 1: Speed calibration data

S. No.	Hz	Free stream flow velocity m/s		
		External balance software	Digital manometer	Mano-meter tube
1	0.0	0.00	0.00	0.00
2	3.0	1.93	2.21	2.70
3	5.0	3.87	3.69	4.04
4	7.5	6.40	6.72	6.67
5	10.0	9.07	9.42	9.30
6	12.5	11.60	12.06	12.07
7	15.0	14.03	14.76	14.77
8	17.5	16.50	17.35	17.42
9	20.0	18.83	20.08	20.15
10	22.5	21.17	22.65	22.82
11	25.0	23.50	25.17	25.45
12	27.5	25.80	27.65	28.00
13	30.0	27.93	30.20	30.41

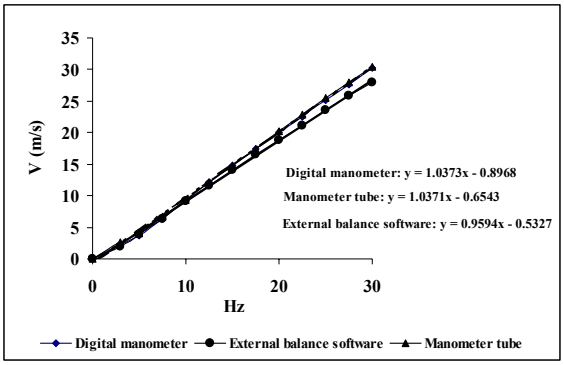

Fig 1: Free stream velocity vs. RPM controller speed.

It is observed that the curves for the digital manometer and the tube manometer readings are practically the same whereas the curve for the data using six component external balance software deviates a little from the other two curves. The experimental error using the external balance is nearly 6%. The flow velocity readings of the external balance are corrected through the following calibration equation obtained through the data shown in figure-2,

$$y = 1.0796x - 0.2336 \quad (1)$$

where x denotes external balance software velocity (m/s) and y denotes digital manometer velocity (m/s).

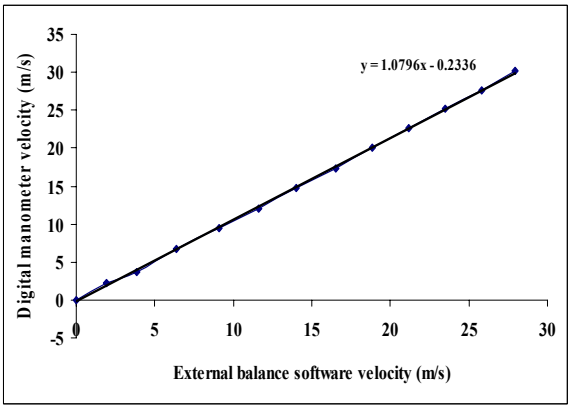

Fig 2: Flow velocity calibration for external balance

Using the equation (1), the actual value of free stream air velocity will be 21.36 m/s for corresponding 20 m/s of air velocity from six-component external balance software.

2.2 Flow Quality

The dynamic pressure is measured using digital manometer at different locations in the test section in YZ-plane by means of a pitot tube for a RPM controller setting of 15 Hz. For different locations of the measurement grid the experiments are repeated three times and the experimental data is given in [18]. The average (mean) dynamic pressure is obtained from the measured dynamic pressure data. The dynamic pressure variations from the mean are calculated in percentage at different locations of YZ-plane. Using these data dynamic pressure variations from the mean (%) versus distance from wind tunnel floor (cm) are plotted in Figure 3. From figure-3 it is observed that the variation of dynamic pressure in the test section is within ± 0.5% which indicates that the there is very good uniformity of flow in the test section of the wind tunnel.

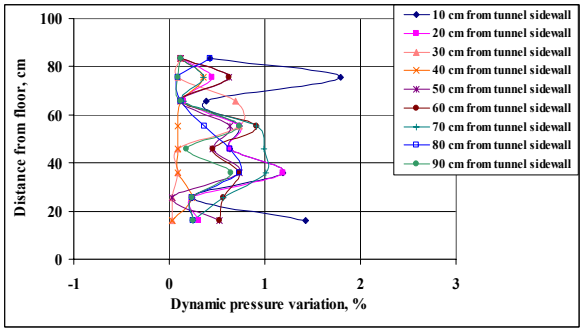

Fig 3: Dynamic pressure variation in the test section.

2.3 Wind Tunnel Model details

The wind tunnel test aircraft model consists of rectangular wing with NACA section No. 65-3-218-aerofoil 0.66 m span and a 0.121 m chord. Two sets of elliptical and circular shaped winglets were designed of wood for the above wing. Figure-4 shows a

Fig 4: Aircraft model check for 0^0 angle of attack.

photograph of the model aircraft with winglet, which is mounted horizontally in the test section of the wind tunnel. The tests were carried out with free-stream velocities of 21.36 m/s, 26.76 m/s, and 32.15 m/s respectively with and without winglet of different configurations. The ambient pressure, temperature and humidity were recorded using barometer, thermometer, and hygrometer respectively for the evaluation of air density in the laboratory environment. Longitudinal tests were carried out at an angle of attack ranging from zero degree to 14 degrees with an increment of 2 degrees. The coefficient of lift (Table 2), and lift curve slopes data (Table 3) are obtained from the experimental results as per the procedure explained in [18-19].

Table 2: Lift coefficients experimental data

S. No.	Winglet Config-uration	Reynolds Number 10^6	Lift coefficient, C_L		
			Initial Angle of Attack 0^0	Stall Angle of Attack 8^0	Final Angle of Attack 14^0
1	WW	0.17	0.237	0.805	0.657
		0.21	0.259	0.817	0.584
		0.25	0.306	0.879	0.733
2	EW1	0.17	0.299	0.829	0.641
		0.21	0.327	0.889	0.700
		0.25	0.359	0.934	0.713
3	EW2	0.17	0.386	0.930	0.729
		0.21	0.394	0.934	0.815
		0.25	0.416	1.018	0.885
4	CWC1	0.17	0.407	0.852	0.563
		0.21	0.429	0.908	0.715
		0.25	0.430	0.967	0.775
5	CWC2	0.17	0.436	0.939	0.775
		0.21	0.451	0.957	0.737
		0.25	0.487	0.985	0.823

Notifications: WW-Without Winglet; EWC1-Elliptical Winglet, Configuration 1 (0^0 angle); EWC2-Elliptical Winglet, Configuration 2 (60^0 angle); CWC1-Circular Winglet, Configuration 1 (0^0 angle); CWC2-Circular Winglet, Configuration 2 (60^0 angle)

Table 3: Lift curve slopes data

Free stream velocity m/s	Reynolds Number 10^6	Lift curve slopes				
		WW	EWC1	EWC2	CWC1	CWC2
21.36	0.17	3.72	3.83	3.85	3.77	3.76
26.76	0.21	4.01	4.09	4.13	4.03	3.96
32.15	0.25	4.11	4.15	4.36	3.93	3.67

2.4 Calibration of the Balance

Calibration of the six-component balance has been done to check the calibration matrix data provided by the manufacturer. Figure 5 shows a photograph of the calibration rig used for the validation of calibration matrix, which is mounted on the upper platform of the balance in place of model. The relationship between signal readings, L_i and the loads, F_i applied on the calibration rig are given by the following matrix equation, the detailed procedure of calibration is explained elsewhere [18-19]

$$\{L_i\} = [K_{ij}]\ \{F_i\} \qquad (2)$$

Where, $[K_{ij}]$ is the coefficient matrix.
$\{L_i\}$ is the signal matrix.
$\{F_i\}$ is the load matrix.

The calibration matrix is obtained by finding the inverse of K_{ij}, coefficient matrix and it compares well with the calibration matrix data supplied by the manufacturer with six component external balance.

Fig 5: Calibration rig mounted the test section

3. RESULTS AND DISCUSSION

Wind-tunnel measurements using the aircraft model without winglet and with winglet of different configurations as configuration 1 (Winglet inclination at 0^0), and configuration 2 (Winglet inclination at 60^0) were done at Reynolds numbers 0.17×10^6, 0.21×10^6 and 0.25×10^6. The coefficient of lift and coefficient of drag are calculated from the experimental results as per the procedure explained in [18-19].

3.1 Lift Coefficient Characteristics

The coefficient of lift versus angle of attack for the aircraft model with and without winglet studied in the present investigation are shown in Figure 6 for the maximum Reynolds number of 0.25×10^6. From the figure it is observed that the lift increases with increase in angle of attack to a maximum value and thereby decreases with further increase in angle of attack. The initial values of lift coefficient occur at zero angle of attack and the maximum values of the lift coefficient occur at an angle of attack of 8 degrees. Above this angle of attack lift curve begins to decrease with further increase in angle of attack. The reason for a drop in lift coefficient beyond 8 degree angle of attack is probably due to the flow separation, which occurs over the wing surface instead of having a streamlined laminar flow there. The stalling angle happens to be approximately 8^0 for all the Reynolds numbers under the present study. The least square fit lines are drawn through the data obtained for different configurations until angle of attack of 8^0 and the lift curve slopes, $\frac{dC_L}{d\alpha}$ are found as 4.11, 4.15, 4.36, 3.93, and 3.67 respectively. It is observed that the $\frac{dC_L}{d\alpha}$ slope for all the configuration is practically same with only a marginally high slope, a_0 for elliptical winglet of configuration 1 and 2 as compared to the circular winglet and without winglet configuration. The other details of the lift coefficients are given in Table 2.

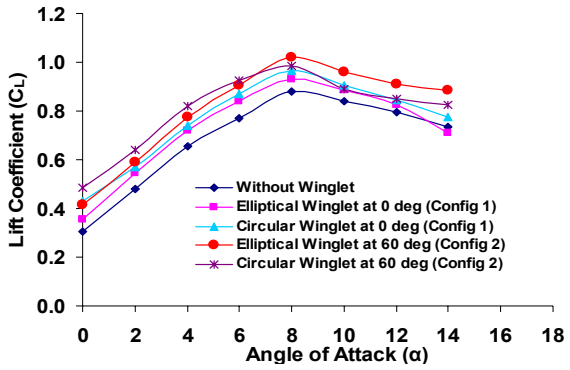

Fig 6: Lift Coefficients for the Aircraft Model

3.2 Lift curve slopes

From the Figure 6 it is observed that the lift curve slope increases with the addition of the winglet (Winglets inclination at 60^0 and 0^0) ranging from 1% to 6% (Table 3) at the maximum Reynolds number of $0.25x10^6$. These experimental results can be explained by comparing with the results obtained at the Georgia Institute of Technology [16]. The tests were run in three configurations: winglets off (Configuration 0), winglets installed at zero degrees (Configuration 1), and winglets deployed at $+20^0$, $+10^0$, 0^0, -10^0, -20^0 (Configuration 2). They showed that flat plate winglets set at zero degrees (Configuration 1) increased lift curve slope by 10% for the maximum Reynolds number of $0.29x10^6$. They also showed that configuration 2 provided the largest increase of lift curve slope, ranging from 15% to 22% increases.

From this investigation it is observed that at the maximum Reynolds number of $0.25x10^6$ elliptical winglet of configuration 1 and 2 (Figure 6) provides the largest increase of lift curve slope, ranging from 1% to 6% increases, giving an edge over other configurations. Decisively it can be said that the elliptical winglet of configuration 2 (Winglets inclination at 60^0) has the better performance giving about 6% increase of lift curve slope as compared to other. Full results of the studies on lift coefficient can be found in Reference [18].

4. CONCULSIONS

Following are the conclusions drawn from this investigation:

The calibration matrix obtained through the interaction matrix method compares well with the matrix data as supplied by the manufactures of the six-component balance.

Aerodynamic characteristics for the aircraft model with and without winglet having NACA wing No. 65-3-218 have been presented.

Elliptical winglet at 60 degree incidence has the better performance giving about 6% increase in lift curve slope and thereby produces more lift as compared to other configurations for the maximum Reynolds number considered in the present study.

5. ACKNOWLEDGEMENT

The authors are grateful for the support provided by grants from the IRPA (Project No: 09-02-04-0446-EA001), and the Aerodynamics Laboratory of Aerospace Engineering Department of the Universiti Putra Malaysia for using the Wind Tunnel.

6. REFERENCES

1. Bento, S. M., Antonini P. M. and Dural H. S. F., 2003, "Considerations about Winglet Design", AIAA Paper-3502.
2. Whitcomb, R. T., 1976, "A Design Approach and Selected Wind-Tunnel Results at High Subsonic Speeds for Wing-Tip Mounted Winglets", NASA N D-8260.
3. Whitcomb, R. T. 1981, "Methods for Reducing Aerodynamic Drag", *NASA* Conference Publication 2211, Proceedings of Dryden Symposium, California
4. Yates, J. E., and Donaldson, C., 1986, "Fundamental Study of Drag and an Assessment of Conventional Drag-Due-To-Lift Reduction Devices", NASA Contract Rep 4004.
5. Louis, B. G., 1992, "Spiroid-Tipped Wing", U. S. patent 5, 102,068.
6. Reginald, V. F., 1978, "Vortex Reducing Wing Tip", U. S. Patent 4, 108, 403.
7. Clark, J., 1999, "Aviation Partners, Inc., Personal Communication".
8. Jones, R. T., 1984, "Improving the Efficiency of Smaller Transport Aircraft", *14th Congress of the International Council of the Aeronautical Sciences*, proceeding, Vol. 1, Toulouse, Fr.
9. Chandrasekharan, R. M., Murphy, W. R., Taverna, F. P., and Boppe, C. W., 1985, "Computational Aerodynamic Design of the Gulftream IV Wing", AIAA-85-0427.
10. Maughmer, M. D., Tmothy, S. S., and Willits, S. M., 2001, "The Design and Testing of a Winglet Airfoil for Low-Speed Aircraft", AIAA Paper 2001-2478.
11 Spillman, J. J., 1978, "The use of wing tip sails to reduce vortex drag", Aeronautical Journal, September, pp. 387-395.
12. Spillman, J. J., Ratcliffe, H. Y., and McVitie, A., 1979, "Flight experiments to evaluate the effect of wing-tip sails on fuel consumption and handling characteristics", Aeronautical Journal, July, pp. 279-281.
13. Spillman, J. J., and Fell, M. J., 1983, "The effects of wing tip devices on (a) the performance of the Bae Jetstream (b) the far-field wake of a Paris Aircraft", Paper 31A, AGARD CP No. 342, Aerodynamics of Vortical Type Flows in Three Dimensions, April, pp. 31A-1-11.
14. Heinz, G. K., 1988, "Auxiliary Wing Tips for an Aircraft", U. S. Patent 4722499, February.
15. Vance A.T., 1993, "Gliding Birds: Reduction f Induced Drag by Wing Tip Slots between the Primary Feathers", Journal of Experimental Biology, Vol. 180 (1), pp. 285-310.

16. Smith, M. J., Komerath, N., Ames, R., Wong, O.,and Pearson, J. , 2001, "Performance Analysis of a Wing with Multiple Winglets", AIAA Paper-2001-2407.

17. Roche, La. U., and Palffy, S., 1996, "WING-GRID, a Novel Device for Reduction of Induced Drag on Wings," Proceedings of ICAS 96, Sorrento, September.
18. Hossain, A., 2005, "Investigations of Longitudinal Aerodynamic Characteristics of Aircraft Model with and without Winglet", M.Sc. Thesis, Universiti Putra Malaysia, UPM Serdang, Malaysia.
19. Prithvi, R. A., Hossain, A., Jaafar, A. A., Edi, P., Younis, T. S., and Saleem, M., 2005, "Drag Reduction in Aircraft Model using Elliptical Winglet", Journal of IEM, Malaysia, Vol. 66, No. 4.

7. NOMENCLATURE

Symbol	Meaning	Unit
p	Absolute pressure	(N/m^2)
T	Temperature	(K)
R	Gas constant	(Nm/kg.K)
ρ_∞	Air density	(kg/m^3)
μ_∞	Air viscosity	(kg/m.s)
v_∞	Free stream velocity	(m/s)
c	Chord length	(m)
Re	Reynolds number	(Dimensionless)
b_1	Blade height	(m)
c_1	Blade width	(m)
S_1	Blade frontal surface area	(m^2)
b_2	Drag height	(m)
c_2	Drag width	(m)
S_2	Drag device frontal surface area	(m^2)
S_T	Total frontal area of wind turbine	(m^2)
P_{wind}	Wind power	(W)